www.czasopisma.pan.pl PAN POLSKA AKADEMIA NAUK www.journals.pan.pl

Arch. Metall. Mater. **64** (2019), 4, 1369-1375

DOI: 10.24425/amm.2019.130103

Ł. WÓJCIK*#, Z. PATER*

PHYSICAL SIMULATION OF THE MANNESMANN EFFECT IN THE ROLLING PROCESS

The study presents the results of laboratory testing of the phenomenon of cracking in the process of cross rolling. A new method of determining the critical value of the damage function was developed, in which a disc-shaped sample is subjected to rotational compression in a channel. In this method the Mannesmann effect was used. The laboratory tests were conducted for C45, 50HS and R260 grade steel in the temperature range 950°C-1150°C. In order to research various methods of simulating the phenomenon of cracking in the process of cross rolling, physical modelling was also employed. The model material was commercial plasticine, cooled to the temperature 0°C-20°C. Comparing the test results for both the real and model material allowed one to determine the range of the forming temperature for the model material, in which the cracking process is similar to the case of the real material.

Keywords: Mannesmann effect, physical modelling, plasticine, crack, cross-rolling process

1. Introduction

Cross rolling is one of the basic plastic forming processes used in manufacturing axial-symmetric products. It can also be employed to manufacture semi-finished products that are later subjected to precise plastic forming or machining. Cross rolling proves beneficial in many aspects, such as its efficiency, obtaining a better shape of the preform, low material waste and a possibility of automatizing the process. Despite those advantages, there are limits to the process, among others: uncontrollable slip of the formed material between the tools, contractions in the formed forgings and the occurrence of internal cracks [1-3].

Shrinkage porosity and internal cracks occurring during the cross rolling process are a result of the Mannesmann effect in the axial area of the formed forging. Internal defects are usually longitudinal axial cracks [4].

The occurrence of the Mannesmann effect (cracking) is influenced by the following factors:

- cyclically changing compressive and tensile stresses,
- gradual damage to the material cohesion as a result of a low-cycle material fatigue,
- a high level of non-metallic inclusions in the formed material [5-8].

In order to examine the occurrence of internal damage to the formed products computer techniques based on previously implemented fracture criteria suitable for the analyzed forming processes are used.

In the computer-based tests a specialist simulating software is applied [9-15]. The programmes used for numerical simulations substitute the real model with a discrete model, consisting of a finite number of elements and nodes. The computer tests allow for obtaining results for forgings of a complex shape. The calculation accuracy, however, is highly dependent on the adopted critical value of the damage function, determined in the so-called calibrating tests [16].

Since in the process of physical modelling the real material is substituted for the model one, there is no need to conduct the tests in industry conditions.

The flow curves for the model material ought to be similar to the ones for real material, whereas the entire physical modelling process should mirror the friction conditions, tool shape (scale) and forming kinematics of the real process. The tools might also be manufactured from the model material [17].

Materials used for physical modelling can be divided into two groups: metallic and non-metallic materials. Non-metallic materials are: resins, natural waxes, synthetic waxes, cellulose, plasticine, plastic (e.g. ABS, PLA, Teflon) and wood, whereas the examples of metallic materials are: aluminium, sodium, lead, tin, copper and Wood's metal.

Recently, the following plastic forming processes have been researched using the physical modelling method: forging, extrusion and rolling [18-29]. Laboratory analysis using physical modelling omitted the problem of modelling the process limitations, mainly the occurrence of internal cracking, which usually renders the final product unsuitable.

* LUBLIN UNIVERSITY OF TECHNOLOGY, 38D NADBYSTRZYCKA STR., 20-618 LUBLIN, POLAND

Corresponding author: l.wojcik@pollub.pl

2. Materials and Methods

An original method of determining the critical value of the damage function by compressing a disc-shaped sample in a channel has been applied in the research. In this method the Mannesmann effect is used, as a result of which axial cracking of the formed material occurs. Figure 1 presents a scheme of the proposed research method. In the research tools with a 8 mm deep channel were used.

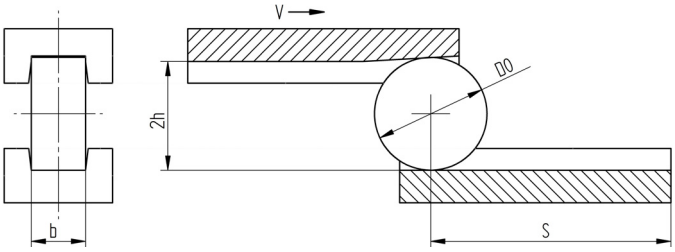

Fig. 1. Scheme of the process of compression in a channel

In this method, the formed disc is placed in a channel at the S distance from the end of the nether tool. The upper tool, set in motion, forms the disc from the initial diameter D0 to the final diameter 2 h, whereas the nether tool remains motionless. An indentation in the front surface of the upper tool enables a proper input of the disc between the tools. Side walls of the channel prevent axial lengthening of the material, which causes the sample to be subjected to changing compressive and tensile stresses, which induces the formation of axial cracks.

Fig. 2. Laboratory cross-wedge rolling mill

In the laboratory testing of steel a cross-wedge rolling mill (Fig. 2), located at the Lublin University of Technology was used. The aforementioned rolling mill can be equipped with tools of the maximum length 1000 mm. A hydraulic drive, allowing the tools to move with the constant speed v = 300 mm/s was used.

The samples used for experimental testing were disc-shaped, with the diameter equal 40 mm, length 20 mm and made of C45, 50HS and R260 type material. Table 1 presents the chemical compositions used for testing materials.

The distance between the nether and upper surface of the channel was set to 2h = 38 mm. The sample were heated in an electric chamber furnace to the temperatures 950°C, 1000°C, 1050°C, 1100°C, 1150°C. Further on, the heated discs were placed in the channel of the nether tool. The test was conducted for various values of the distance S until cracking and the longest distance was selected. The test was then repeated twice for the same parameters. If no cracks were detected after subjecting the samples to the rolling process three times, distance S was deemed the limit distance value.

In order to examine various methods for simulating the cracking phenomenon in the process of cross rolling, physical testing was also conducted, using commercial plasticine as the model material. In the experiment, commercial plasticine PRIMO manufactured by Morocolor (two types of plasticine, here called white and black) was used.

Plasticine is a model material comprising of a mixture of clays, oils, waxes and colouring pigments. Therefore it is perceived as a non-metallic model material [30].

The plasticine used for physical tests was subjected to plastometric tests [31], as a result of which the equations (1) and (2), describing the model material, were obtained:

- White plasticine:

$$\sigma_F = 0,4806\varepsilon^{-0,0313} e^{0,08705\varepsilon} \dot{\varepsilon}^{\left(0,2451+(-0,0026)T\right)} e^{-0,03283T} \quad (1)$$

- Black plasticine:

$$\sigma_F = 0,6817\varepsilon^{-0,0711} e^{0,07203\varepsilon} \dot{\varepsilon}^{\left(0,2701+(-0,0037)T\right)} e^{-0,07358T} \quad (2)$$

where: σ_F – flow stress [MPa], ε – strain [-], $\dot{\varepsilon}$ – strain rate [1/s], T – temperature [°C].

Model material was also examined in order to determine the limit value of the Cockroft-Latham integral [31]. The values obtained in the tension test were compared to the graphical values of hot forming for steel. A similarity between the limit value of the Cockroft-Latham integral for white plasticine, formed in the temperature range 0°C to 5 °C, black plasticine, formed in 0°C and C45 grade steel, hot formed in the temperature range

TABLE 1

Percentage chemical compositions used for testing materials

Grade steel	C	Mn	Si	P max	S max	Cr max	Ni max	Mo max	Cu max
C45	0,42-0,5	0,5-0,8	0,1-0,4	0,04	0,04	0,3	0,3	0,1	0,3
50 HS	0,45-0,55	0,3-0,6	0,8-1,2	0,03	0,03	0,9-1,2	0,4	—	0,25
R260	0,62-0,8	0,7-1,2	0,15-0,58	0,025	0,008-0,025	—	—	—	—

900°C-1200°C was observed. The limit values of the Cockroft-Latham integral, for C45 grade steel in this temperature range oscillate around 0,849÷0,726, for white plasticine formed in the temperature range 0°C-5°C is equal 0,850÷0,646, whereas for black plasticine in 0°C it is equal 0,691.

Commercial plasticine has also been tested in order to determine the friction factor and friction coefficient between the ABS tools and model material. The tests showed a similarity of friction conditions in the case of deforming white and black plasticine and hot-forming of steel [32].

Physical testing was conducted in a lab stand (Fig. 3) developed in the laboratory of the Department of Computer Modelling and Metal Forming Technologies of Lublin University of Technology. The lab stand was based on a laboratory chain drawing machine. The machine enables the change of the linear speed of the tools in the range 0 to 150 mm/s. Moreover it is equipped with a measurement system AXIS FC1K – dynamometer registering data with the maximum force range 1 kN. The module of the model cross-wedge rolling mill allows for using 3D printed 1:2 and 1:2.5 scale model tools.

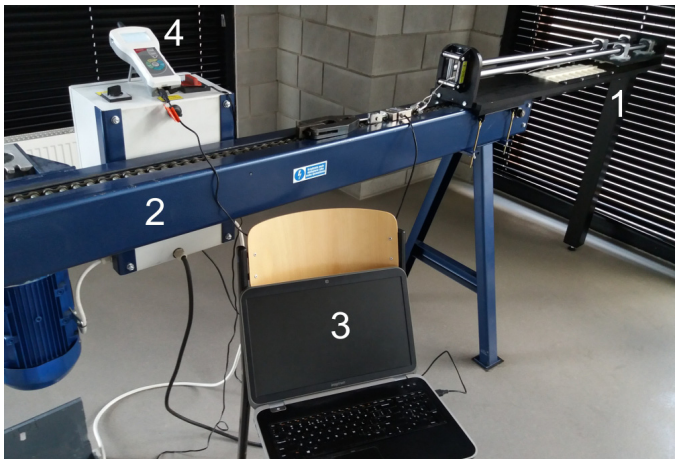

Fig. 3. Model cross-wedge rolling mill : 1 – model module, 2 – chain drawing machine, 3 – computer with the software, 4 – AXIS measurement system

Test tools were 3D printed from ABS. A 3D printer uPrint SE, employing the FDM method in which thin layers of the melted material are applied. The tools were assembled from two segments (Fig. 4.)

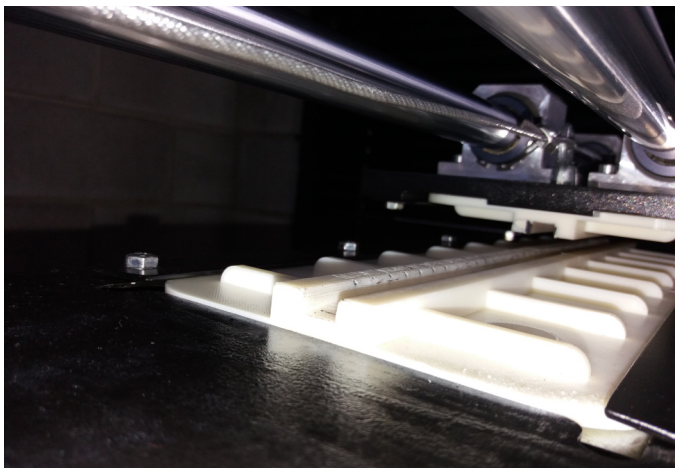

Fig. 4. Model tools mounted in the model rolling mill

In specialist literature various methods of sample preparation were presented. Based on the discussed methods, an original method of sample preparation was developed [33-36], in which four main stages can be distinguished. At first, the portions of plasticine were heated to 30-35°C, the material was manually deformed several times in order to eliminate air bubbles that could negatively influence the quality of the sample. In the second stage cylindrical bars were extruded, with the diameter 20 mm, whereas in the next stage they were divided in to 10 mm – long discs. In the last stage the samples were placed in a cooler in the temperature range 0-20°C for 24 h. Such time allowed one to obtain a similar temperature of the samples in their entire volume.

Model testing was conducted similarly to the real process using hot-formed steel. The model samples, tools and the linear speed were 1:2 scale models.

During the real and model tests changes to the force in the time of sample forming were registered.

3. Results and discussion

Based on the results of the real and model tests of the process of compression in a channel the limit values of the forming distance and the number of rotations of the samples were determined.

In the Table 2 below the limit values of the distance, upon exceeding which the cracking occurs, are presented.

TABLE 2

Limit values of the distance

Steel temperature T [°C]	Limit length S [mm]			Plasticine temperature T [°C]	Limit length S [mm]			
	C45 Steel	50HS Steel	R260 Steel		White Plasticine		Black Plasticine	
					Real	Scale 2:1	Real	Scale 2:1
950	220	150	225	0	145	290	150	300
1000	230	175	250	5	160	320	160	320
1050	350	185	375	10	180	360	170	340
1100	430	275	500	12	240	480	190	380
1150	675	325	550	15	—	—	240	480
				20	—	—	290	580

$$n = \frac{S}{\pi \cdot D_0} \tag{3}$$

where: S – distance from the end of the nether tool [mm], D_0 – initial diameter of the tool [mm],

Another task was conducting calculations in accordance with the formula (3), based on which a critical number of the rotations of the sample, upon exceeding which the cracking occurred was determined. The results of the calculations are presented in Table 3.

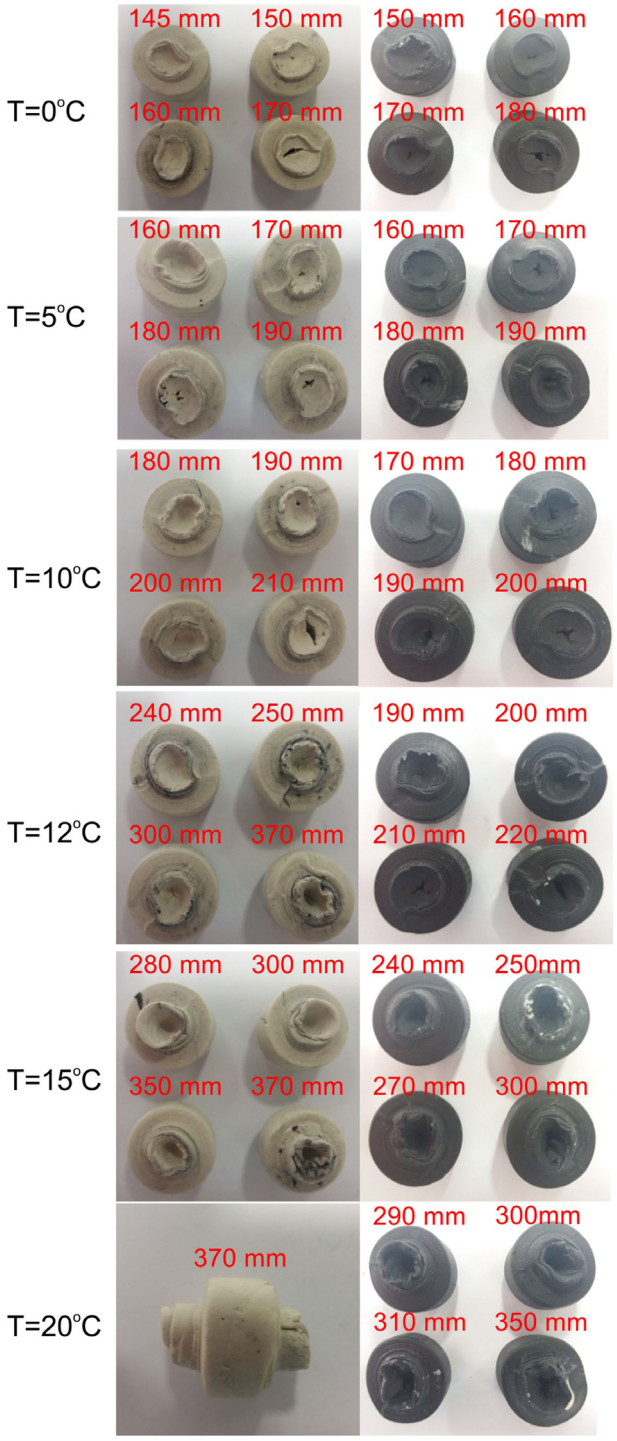

Fig. 5. Samples of the material model after rotary compression test (RTC)

TABLE 3

Critical number of the rotations of the sample upon exceeding which the cracking occurs

Steel temperature T [°C]	C45 Steel	50HS Steel	R260 Steel	Plasticine temperature T [°C]	White plasticine	Black plasticine
950	1,75	1,19	1,79	0	2,28	2,39
1000	1,83	1,39	1,99	5	2,55	2,55
1050	2,79	1,47	2,98	10	2,86	2,71
1100	3,42	2,19	3,98	12	3,82	3,025
1150	5,37	2,59	4,38	15	—	3,82
				20	—	4,62

Figure 5 presents the photographs of the obtained model samples divided based on the type of plasticine and temperatures of compression. The samples were organized by the incremental order of the forming path.

It was also observed that white plasticine cracks in the following temperatures: 0, 5, 10, 12°C, whereas at 15°C and 20°C the model tools proved to be too short – the formed material flowed through the spaces between the tools.

Black plasticine cracked in the entire temperature range.

Figures 6-8 show samples of C45, 50HS and R260 grade steel after laboratory testing. The samples were organized by the forming temperature and the incremental order of the forming path.

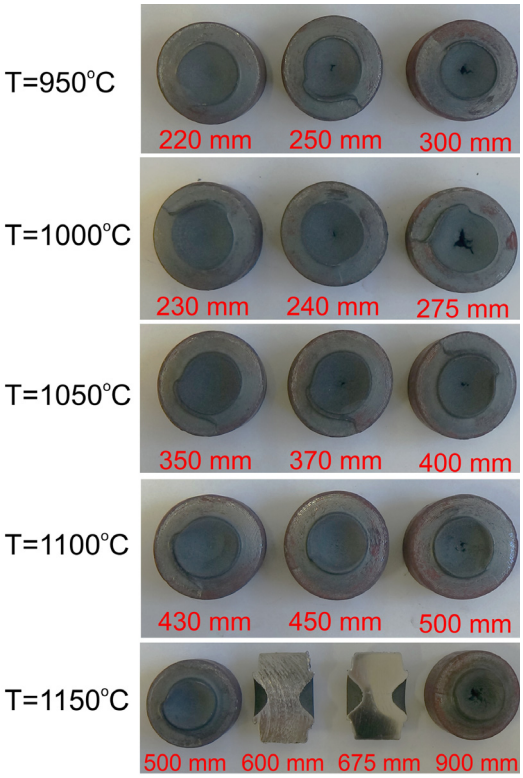

Fig. 6. C45 grade steel samples after RTC

The length of the forming path increased along with the increase of the temperature of the samples, whereas the cracking grew less visible (porosity shrinkage occurred).

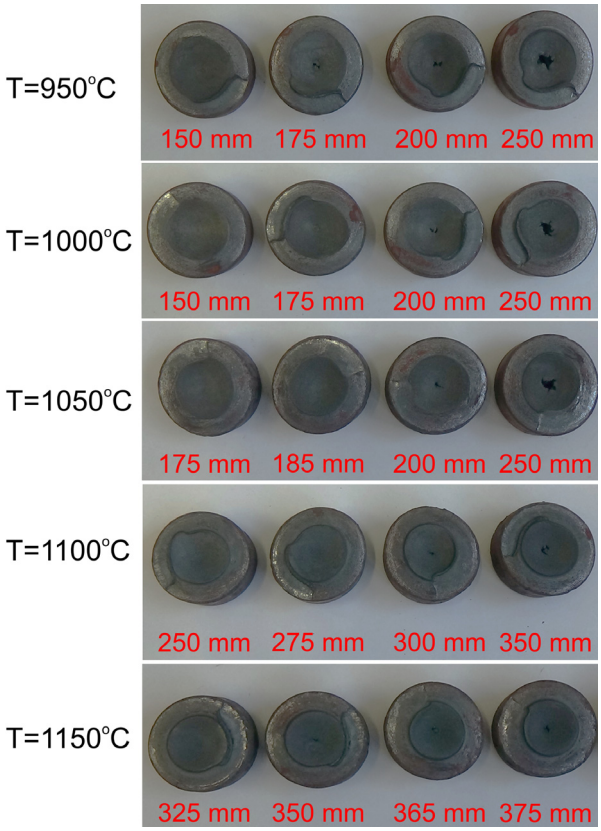

Fig. 7. 50HS grade steel samples after RTC

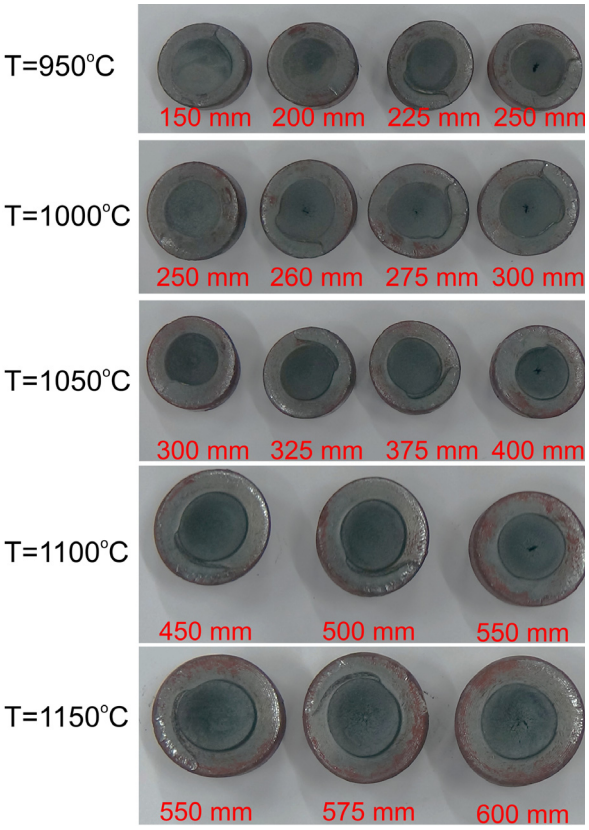

Fig. 8. R260 grade steel samples after RTC

Figure 9 presents the critical number of rotations in a chart form, allowing one to view the forming temperature of the model materials. This temperature mirrors the cracking of steel in the selected temperatures of the real material forming.

Based on the chart, the forming temperatures for the model materials mirroring the process of compression of a C45 grade steel sample in the forming temperature $T = 1050°C$. White plasticine is the best model material for the compression of a C 45 grade steel sample formed in the temperature $T = 9°C$, whereas black plasticine $T = 11°C$

Further on, calculations aiming to determine the similarity coefficient between the model materials and the real material in the selected conditions. The similarity coefficient was determined based on the formula (4).

$$\lambda = \frac{\int_0^1 \sigma_{F\ steel}\, d\varepsilon}{\int_0^1 \sigma_{F\ plast}\, d\varepsilon} \tag{4}$$

where: $\sigma_{F\ steel}$ – flow stress of steel [MPa], $\sigma_{F\ plast}$ – flow stress of plasticine [MPa].

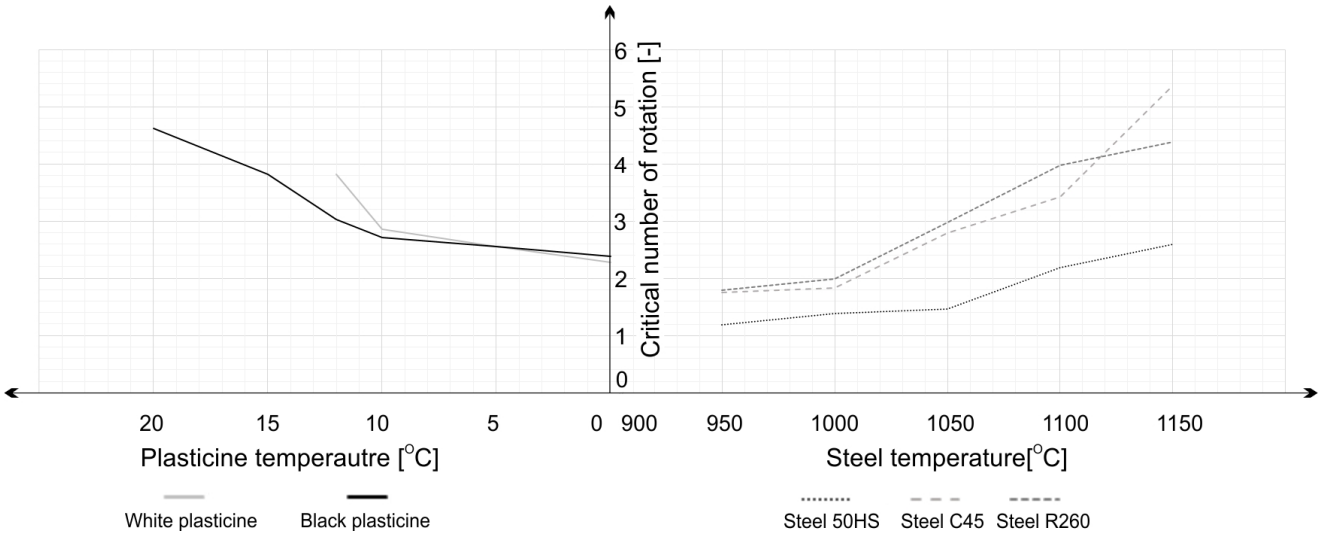

Fig. 9. Change to the critical number of rotations

The values of the obtained similarity factors are presented in Table 4.

TABLE 4

Similarity factor values

Similarity factor λ	White plasticine	Black Plasticine
Steel C45 $T = 1050°C$	$T = 9°C$	$T = 11°C$
	223,6	263

Subsequently model testing was conducted, which resulted in obtaining the force progress. It was observed that the shape of the force progress for the real material is similar to the forces occurring during the process of model material forming (Fig. 10).

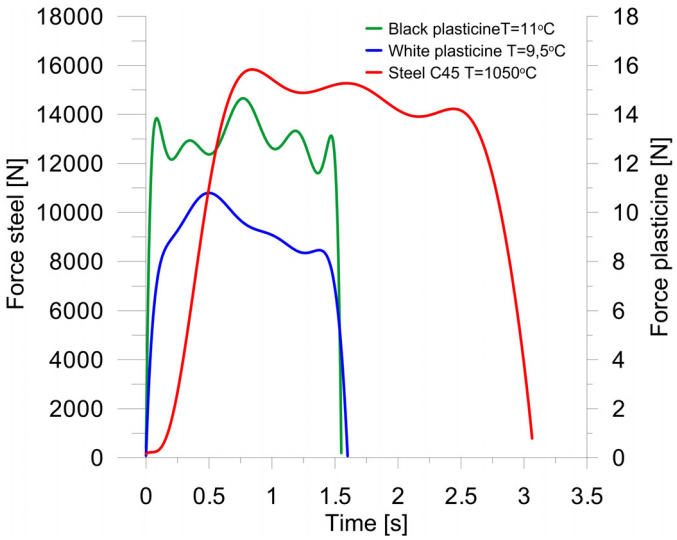

Fig. 10. Progression of the forming forces

The final stage was determining the estimated value of the real force of forming the C45 grade steel in $T = 1050°C$. The real force was estimated based on the formula (5).

$$F = \lambda F' s^2 \tag{5}$$

where: F' – Forming force from model testing [N]; λ – Similarity factor of the plasticity of the model material [-], s – scale of the tools.

The forming force determined by the model testing was assumed, respectively 9 N for white plasticine and 16 N for black plasticine, tool scale equal 2. The following results were obtained: for white plasticine $F = 8,3$ kN and for black plasticine $F = 13,6$ kN, whereas for C45 grade steel the real force was equal $F = 14$ kN. The estimated force for white plasticine was 41% less significant than the real force, whereas for black plasticine 3%.

Upon analysing the results it was stated that the estimated forming force for the black plasticine is the most similar to the force obtained in real testing.

4. Conclusions

Comparison of the results obtained in real and model laboratory testing allowed one to determine the temperature ranges for the model materials, in which the cracking process of the real material in the selected forming temperature range is mirrored.

The limit forming path in 0°C for black plasticine is 3% shorter compared to that of white plasticine. For the temperatures 10 and 12°C the limit forming path for black plasticine is shorter by, respectively, 5,5% and 20,8% compared to white plasticine. At 5°C the limit forming path is similar for both types of plasticine. The conducted real and model tests confirmed the possibility of using commercial black and white plasticine as a model material for physical testing. In the case of physical modelling, the forming process of C45 grade steel at 1050°C is best modelled with black plasticine, for which the forming force value is only 3% smaller than the one of the real process.

The obtained results allow for determining the conditions of the physical modelling of the cross-rolling process, in which the cracking caused by the Mannesmann effect might occur.

It was also stated that physical modelling enables one to precisely determine the values of forces occurring in the cross-rolling process.

Acknowledgements

The research has been conducted under the project No. 2017/25/B/ST8/00294 financed by the National Science Centre, Poland.

REFERENCES

[1] Z. Pater, Walcowanie poprzeczno-klinowe, Lublin (2009).
[2] M. Skripalenko, B. Romantsev, S. Galkin, M. Skripalenko, L. Kaputkina, T. Huy, Metallurgist. **61** (11-12), 925-933 (2018).
[3] G.V. Kozhevnikova, Theory and Practice of Cross-Wedge Rolling, Minsk (2010).
[4] A. Ghiotti, S. Fanini, S. Bruschi, P.F. Bariani, CIRP Annals – Manufacturing Technology **58**, 255-258 (2009).
[5] G. Liu, Z. Zhong, Z. Shen, Procedia Engineer. **81**, 263-267 (2014).
[6] Y. Dong, K.A. Tagavi, M.R. Lovell, Z. Deng, Int. J. Mech. Sci. **42**, 1233-1253 (2000).
[7] G. Liu, G. Ren, C. Xu, Z. Jiang, Z. Shen, J. Mech. Eng. **20** (2), 150-152 (2004).
[8] G. Fang, L.P. Lei, P. Zeng, J. Mater. Process. Tech. **129**, 245-249 (2002).
[9] K. Mori, H. Yoshimura, K. Osakada, J. Mater. Process. Tech. **80-81**, 700-706 (1998).
[10] M.-S. Joun, J. Lee, J.-M. Cho, S.-W. Jeong, H.-K. Moon, Procedia Engineer. **81**, 197-202 (2014).
[11] H.W. Lee, G.A. Lee, D.J. Yoon, S. Choi, K.H. Na, M.Y. Hwang, J. Mater. Process. Tech. **201**, 112-117 (2008).

[12] F.-J. Wang, Y.-H. Shuang, J.-H. Hu, G.-H. Wang, J.-C. Sun, J. Mater. Process. Tech. **214**, 1597-1604 (2014).
[13] T. Komischke, P. Hora, G. Domani, M. Plamondon, R. Kaufann, Procedia Manufacturing **15**, 176-184 (2018).
[14] Z. Pater, Ł. Wójcik, P. Walczuk, Advances in Science and Technology Research Journal **10**, 752-757 (2011).
[15] M.F. Novella, A. Ghiotti, S. Bruschi, P.F. Bariani, Procedia Engineer. **81**, 221-226 (2014).
[16] M.F. Novella, A. Ghiotti, S. Bruschi, P.F. Bariani, J. Mater. Process. Tech. **222**, 259-267 (2015).
[17] L. Kowalczyk, Modelowanie fizykalne procesów obróbki plastycznej, Radom (1995).
[18] Y.H. Moon, C.J. Van Tyne, J. Mater. Process. Tech. **99**, 185-190 (2000).
[19] J. Rasty, H. Sofuoglu, Tribol. Int. **33**, 523-529 (2000).
[20] M. Arentoft, Z. Gronostajski, A. Niechajowicz, T. Wanheim, J. Mater. Process. Tech. **106**, 2-7 (2000).
[21] Z.C. Sun, J. Cao, H.-L. Wu, Z.-K.Yin, Int. J. Adv. Manuf. Tech. **98**, 2933-2942 (2018).
[22] B. Krishnamurthy, O. Bylya, K. Davey, Procedia Engineer. **207**, 1075-1080 (2017).
[23] W. Zhou, J. Lin, T.A. Dean, L.Wang, Int. J. Mach. Tool. Manu. **126**, 27-43 (2018).
[24] I. Balasundar, M. Sudhakara Rao, T. Raghu, Material and Design **30**, 1050-1059 (2009).
[25] D.I. Buteler, P.C.U. Neves, L.V. Ramos, C.E.R. Santos, R.M. Souza, A. Sinatora, J. Mater. Process. Tech. **179**, 50-55 (2006).
[26] Y.-M. Hwang, W.M. Tsai, F.H. Tsai, I Her. Int. J. Mach. Tool. Manu. **46**, 1555-1562 (2006).
[27] J.R. Cho, W.B. Bae, Y.H. Kim, S.S. Choi, D.K. Kim, J. Mater. Process. Tech. **80-81**, 161-165 (1998).
[28] Y. Dong, M. Lovell, K. Tagavi, J. Mater. Process. Tech. **80-81**, 273-281 (1998).
[29] M.M. Skripalenko, E. Bazhenov, B.A. Romantsev, M.N. Skripalenko, T.B. Huy, Y.A. Gladkov, Mater. Sci. Tech. **32** (16), 1712-1720 (2016).
[30] Ł. Wójcik, K. Lis, Z. Pater, Open Engineering, **6** (1), 653-659 (2016).
[31] Ł. Wójcik, Z. Pater, Acta Mechanica et Automatic **12** (4), 286-293 (2018).
[32] Ł. Wójcik, Z. Pater, Hutnik Wiadomości Hutnicze **85**, 362-366 (2018).
[33] A. Asswmpour, S. Razi, J. Mech. Eng. **4** (1), 61-69 (2003).
[34] V. Vazquez, T. Altan, J. Mater. Process. Tech. **98**, 212-223 (2000).
[35] A.E.M. Pertence, P.R. Cetlin, J. Mater. Process. Tech. **84**, 261-267 (1998).
[36] A. Segawa, T. Kawanami, J. Mater. Process. Tech. **47**, 375-384 (1995).